# Paper-based potentiometric sensing of free bilirubin in blood serum

Jeffrey G. Bell[a], Maral P.S. Mousavi[a], Mohamed K. Abd El-Rahman[a,b], Edward K.W. Tan[a,c], Shervanthi Homer-Vanniasinkam[d,e,f], George M. Whitesides[a,g,h,*]

[a] Department of Chemistry and Chemical Biology, Harvard University, 12 Oxford Street, MA 02138, United States
[b] Department of Analytical Chemistry, Faculty of Pharmacy, Cairo University, Kasr-El Ani Street, Cairo 11562, Egypt
[c] Department of Engineering, University of Cambridge, Cambridge CB3 0FA, UK
[d] Leeds Vascular Institute, Leeds General Infirmary, Leeds, UK
[e] Department of Mechanical Engineering and Division of Surgery, University College London, London, UK
[f] Division of Surgery, University of Warwick, Coventry, UK
[g] Kavli Institute for Bionano Inspired Science and Technology, School of Engineering and Applied Sciences, Harvard University, 29 Oxford Street, MA 02138, United States
[h] Wyss Institute for Biologically Inspired Engineering, Harvard University, 60 Oxford Street, MA 02138, United States

## ARTICLE INFO

## ABSTRACT

Bilirubin is predominantly formed in the liver as a result of breakdown of hemoglobin. Knowing the concentration of bilirubin in serum is important in evaluating the health of the liver, and for the diagnosis of hyperbilirubinemia (a condition that afflicts approximately 60% of full-term and 80% of pre-term newborns). This paper describes the design and fabrication of a potentiometric sensor for the determination of free bilirubin in serum. The sensor has a polymeric ion-selective membrane, and selectively measures free ionic bilirubin ("unbound" bilirubin – i.e., bilirubin not complexed to albumin or other complexing agents), in the presence of other anions — chloride, phosphate, pyruvate, deoxycholate, and lactate — also present in serum. The linear response range of the sensor (1.0 mM to 0.10 μM bilirubin, measured in a sodium phosphate buffer with pH 8.6) covers the clinically-relevant concentration of bilirubin in serum (5–500 μM). Free bilirubin could be detected in human blood serum with this potentiometric sensor. The components of the potentiometric bilirubin sensor were embedded in a paper-based device to provide a sensor that is disposable and easy to use, and thus is suitable for applications at the point-of-care. The paper-based potentiometric bilirubin sensor exhibited a response range of 5.0–0.10 mM (sufficient to cover the clinically-relevant concentration of bilirubin in serum). Only 15 μL of sample is required for measurement of the concentration of free bilirubin, and the analysis can be performed in less than two minutes.

## 1. Introduction

The amount of bilirubin (BR) in biological fluids (i.e., blood and urine) is a key indicator of liver health (Lopez-Velazquez et al., 2014). Bilirubin is a tetrapyrrole (Scheme 1) formed by catabolism of heme; it is present in human fluids either complexed with albumin, conjugated with glucuronic acid or free (Kapitulnik, 2004; Ryoichi et al., 2018). Free BR has a pH-dependent solubility, and can deposit in tissues (Erlinger et al., 2014). In healthy adults, the normal concentration of free BR in serum is from 5 to 34 μM; however, in newborns suffering from hyperbilirubinemia, the concentration of BR reaches concentrations as high as 500 μM (Balamurugan and Berchmans, 2015). Determining the concentration of free bilirubin in serum is particularly important in cases of hyperbilirubinemia (a condition which effects approximately 60% of full-term and 80% of pre-term newborns)

(Ahlfors et al., 2009). This importance reflects the fact that acute bilirubin encephalopathy (where BR crosses the blood-brain barrier and can cause irreversible neurological damage) has been found in jaundiced newborns with normal levels of total BR, but high levels of free BR (Ahlfors et al., 2009). Analysis of free BR at the point-of-care (PoC) would facilitate treatment protocols that minimize the risk of long-term brain damage or death.

Most of deaths stemming from hyperbilirubinemia occur in low-resource regions, where it is largely detected based on visual identification of jaundice (i.e., yellowing of the whites of the eyes or the skin). Visual detection is neither quantitative nor reliable (Keahey et al., 2017; Moyer et al., 2000). Analytical methods for quantification of BR include fluorimetry (Santhosh et al., 2014), voltammetry and amperometry (monitoring redox reaction of BR at an electrode surface) (Balamurugan and Berchmans, 2015; Joseph and Mebmet, 1990),
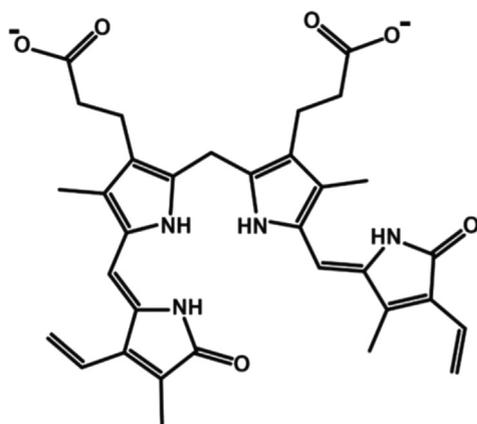
Scheme 1. The structure of bilirubin (net charge of −2).

enzymatic sensors (using bilirubin oxidase) (Doumas et al., 1987; Joseph and Mebmet, 1990; Shoham et al., 1995), chemiluminescence (Lu et al., 2004), high performance liquid chromatography (Ma et al., 2014), piezoelectricity (Yang et al., 2012) and capillary electrophoresis (Nie and Fung, 2008). The three most common methods of BR detection are: (i) conjugation of BR to a diazotized sulfanilic acid followed by analysis by UV–VIS spectrometry (a technique which is highly influenced by pH) (Li and Rosenzweig, 1997; Rand and Pasqua, 1962), (ii) the direct spectroscopic method (which suffers from interference of other heme containing proteins and does not quantify free BR) (Doumas et al., 1987), and transcutaneous bilirubinometry (a skin reflectance technique, which is the gold-standard method employed in hospitals and has been shown to be influenced by skin pigmentation) (Ho et al., 2006; Yamanouchi et al., 1980). Table S1 in the Supporting Information lists various techniques and relevant analytical information for bilirubin detection. For several reasons, these methods are not suitable for rapid, reliable, and affordable quantification of free BR at the point-of-care and in resource-limited settings: (i) They cannot quantify free BR, and measure the total BR (complexed and free). (ii) They require complicated and expensive instruments. (iii) They involve multiple steps of sample preparation and separation, and thus should be performed by skilled personnel. (iv) They require expensive and unstable reagents (i.e., bilirubin oxidase loses 50% of its activity after 17 h at 37 °C) (Shoham et al., 1995).

This work developed a potentiometric sensor using a polymeric ion-selective membrane (ISM) for quantification of free BR in serum. Potentiometry has not been employed for detection of BR prior to this work. Potentiometric sensors (with a polymeric ion-selective membrane) are suitable for affordable point-of-care detection of free BR for five reasons: (i) They have inherent selectivity for detection of lipophilic ions and thus can selectively detect the highly lipophilic BR (Buhlmann and Chen, 2012; Hahm et al., 1992; Lindner and Gyurcsányi, 2009; Lindner and Pendley, 2013) in the presence of less lipophilic ions present in serum, with no need for separation steps. (ii) They can differentiate between the free and complexed ions, and selectively respond to the free ions (Maurer-Jones et al., 2013; Mousavi et al., 2015), and thus can detect free BR in serum. (iii) They have short response times (usually less than 1 s), and can thus provide rapid analysis of BR. (iv) Their sensing components can be integrated in low-cost materials (such as paper and thread) and devices to provide sensors that are affordable and disposable for detection of BR in resource-limited settings (Hu et al., 2016a; Lan et al., 2014; Mousavi et al., 2018; Novell et al., 2012; Ruecha et al., 2017; Szűcs and Gyurcsányi, 2012). (v) They require simple equipment for the readout of signal (a potentiometer for measuring electrical voltage), and thus can be interfaced with the reported low-cost portable potentiometers (Ainla et al., 2018; Jeanneret et al., 2015; Nemiroski et al., 2014).

This work demonstrates selective and enzyme-free detection of free BR in human blood serum with a potentiometric sensor based on an ion-selective electrode (BR ISE). We integrated the components of the BR ISE into a paper-based potentiometric sensor that requires only 15 µL of serum for the analysis.

## 2. Experimental

### 2.1. Materials

Tridodecylmethylammonium chloride (TDMACl), bis(ethylhexyl) sebacate (DOS), high molecular-weight poly(vinyl chloride) (PVC), and blood serum (from human male AB plasma, USA origin, sterile-filtered) were purchased from Sigma-Aldrich. Bilirubin was purchased from Toronto Chemical Research. The Supporting Information (SI) lists the suppliers of other chemicals used in this work.

### 2.2. Fabrication of the BR ISE

We prepared the ion-selective membrane (ISM) by mixing of 990 mg of PVC, 1980 mg of DOS, 15 mg of TDMACl, and 8 mL of tetrahydrofuran (THF). We stirred the mixture until it became homogenous, poured it into a Petri dish (with diameter of 5 cm), and left it covered overnight; this procedure allowed the THF to evaporate, and formed the ISM that provided the ISE. We cut a circular piece of the ISM (diameter of ~1.1 cm and thickness of ~1.2 mm), placed it onto the end of a PVC tube which was wet with THF, and pressed on it for five minutes, this procedure allowed the ISM to fuse to the PVC tube. We filled the PVC tube with 2 mL of a solution (the inner-filling solution (IFS)) containing 0.5 mM BR and 15 mM NaCl in 20 mM sodium phosphate buffer (pH 8.6) inserted an AgCl-coated Ag wire in the tube, and sealed the tube with Parafilm. We placed the electrode in an aqueous solution of 0.5 mM BR (sodium phosphate buffer with pH 8.6) for three hours, followed by immersion in a 10-µM solution of BR for another three hours prior to the analysis to allow exchange of Cl⁻ in the ISM with $BR^{2-}$ (necessary for proper function of the ISE). We fabricated the paper-based potentiometric device according to a previously published procedure (Lan et al., 2014); the SI lists the procedure in detail.

### 2.3. Measurements in serum

We prepared the serum-containing solutions by diluting 1 mL of serum in 9 mL of sodium phosphate buffer (pH of 8.6) containing the desired concentrations of BR (500 µM, 250 µM, and 125 µM).

## 3. Results and discussion

### 3.1. Mechanism of sensing

Potentiometric sensing with ISEs can be used for detection of ionic compounds (Buhlmann and Chen, 2012). BR can be detected using potentiometry because it is doubly charged at values near physiological pH. More than 99% of BR has a −2 net charge at pH values of 7–8.6; $pKa_1 = 4.2$, $pKa_2 = 4.9$; Scheme 1 shows the structure of BR (Boiadjiev et al., 2004). Fig. 1A shows the experimental setup employed in this work for potentiometric measurements. This setup consists of a reference electrode (which provides a sample-independent, and constant, electrical potential), and the ion-selective electrode (ISE). A potentiometer measures the difference between the electrical potential of these two electrodes (the electromotive force or emf). The component of the ISE that provides selectivity is the ion-selective membrane (ISM). The ISM consists of a polymer (poly(vinyl chloride), PVC) to provide mechanical support for the membrane, a plasticizer (bis(ethylhexyl)sebacate, DOS) to dissolve the membrane components and provide ion mobility in the ISM, and a lipophilic ion-exchanging cation (tridodecylmethylammonium, TDMA), which establishes a constant
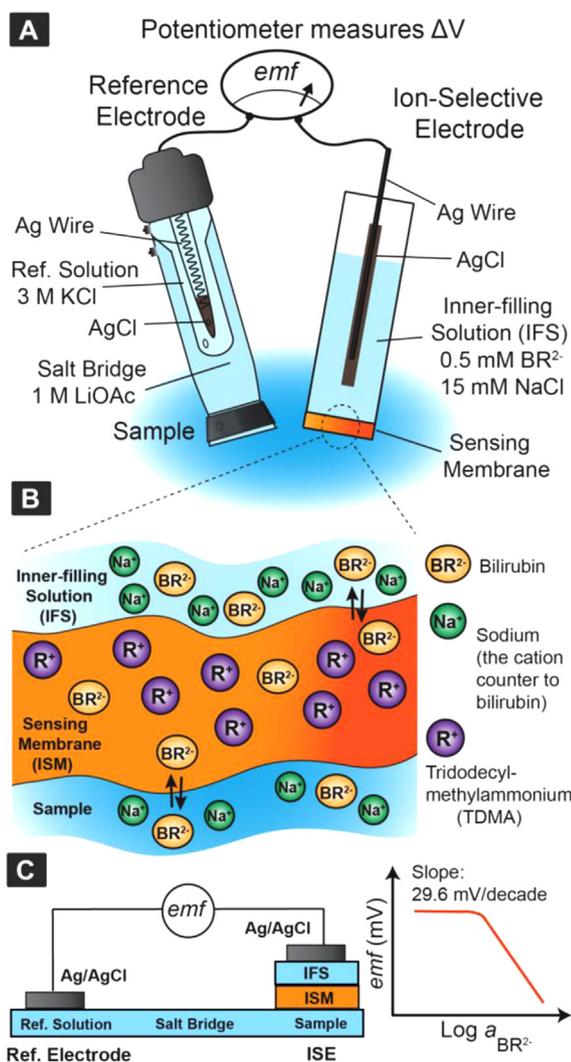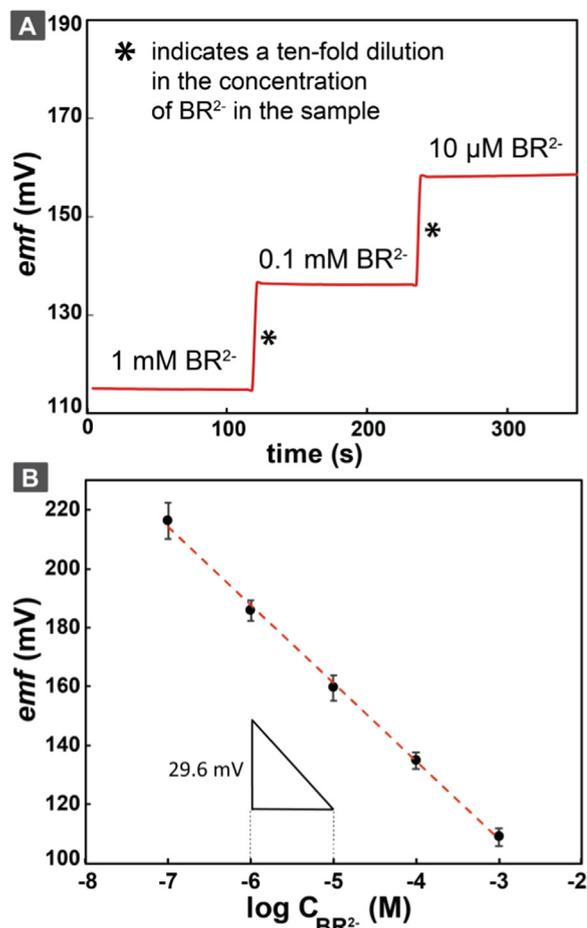
**Fig. 1.** A. The experimental setup for potentiometric measurements with ISEs. B. The components of the sensing membrane (ISM). C. The interfaces involved in the measurement of the *emf* and the theoretically-expected Nernstian response of ISEs.



**Fig. 2.** A. The *emf* of the BR ISE at different concentrations of BR (1 mM, 0.1 mM, and 10 μM) in a sodium phosphate buffer (pH = 8.6). The asterisks show a ten-fold dilution step for changing the concentration of BR in the sample. B. The linear response of the BR ISE (made through successive dilutions) in a concentration range of 1.0 mM–0.10 μM BR in a sodium phosphate buffer (pH = 8.6). We show the average and standard deviation of seven replications (sensor-to-sensor reproducibility was 4 mV in 1 mM BR). The triangle represents the theoretically-expected Nernstian slope (29.6 mV increase in *emf* upon an order of magnitude change in concentration of $BR^{2-}$).

concentration of $BR^{2-}$ in the ISM (Fig. 1B).

The ISM is sandwiched between the sample solution and the inner-filling solution (IFS) which is an aqueous solution containing a constant concentration of $BR^{2-}$ and $Cl^-$. An AgCl-coated Ag wire is immersed in the IFS, and is connected to the potentiometer for the measurement of *emf*. Fig. 1C shows how the sensing components contact each other. The sensing mechanism relies on the creation of a separation of charges ($BR^{2-}$ and $Na^+$) at the interface of the ISM and sample (which creates an electrical voltage at this interface). This electrical voltage depends on the activity of $BR^{2-}$ in the sample. The *emf* is the sum of all interfacial potentials (which all are approximately constant, except for the interface of the ISM and sample) and is given by the Nernst equation (Eq. (1)) (Buhlmann and Chen, 2012),

$$emf = E^0 + \frac{RT}{zF}\ln a = E^0 + \frac{59.2\ mV}{z}\log a \qquad (1)$$

where E° (mV) is the standard potential, R is the gas constant, T is the temperature, F is Faraday's constant, z is the charge of the BR ($-2$ at pH of 8.6), and *a* is the activity of BR. At room temperature, a ten-fold decrease in the activity of BR should (theoretically) increase the *emf* by 29.6 mV (referred to as a Nernstian response) (Buhlmann and Chen, 2012; Lindner and Pendley, 2013).

### 3.2. Response of the BR ISE

We fabricated the potentiometric bilirubin sensor (BR ISE) as shown in Fig. 1A (the Experimental Section discusses the details of fabrication). Fig. 2A shows the *emf* of this ISE at different concentrations of BR in a sodium phosphate buffer with a pH of 8.6. Because the phosphate buffer maintains a constant ionic strength for the measuring solutions, we could assume a constant activity coefficient for the BR, and plot the *emf* vs. concentration (rather than activity) of BR (Bard and Faulkner, 2009). We chose the pH value of 8.6 for the buffer because BR is highly soluble in alkaline aqueous solutions and more than 99% of BR is ionized with a net charge of $-2$ at this pH (Hahm et al., 1992). The ISE exhibited a short response time ($< 1$ s) and the *emf* increased immediately after performing a dilution to decrease the concentration of BR in the sample (our quantification of the response time was limited by how rapidly we could perform the dilutions). Fig. 2B shows the linear response of the BR ISE over five orders of magnitude in a range of concentration of BR (0.10 μM–1.0 mM BR). The slope of *emf* (mV) vs. the logarithm of concentration of BR (M) was $-26.5$ mV/decade, which is close to the theoretically expected slope of $-29.6$ mV/decade. This linear range is sufficient to cover the clinically-relevant concentration range of free BR in healthy patients, and in patients suffering from

hyperbilirubinemia (30–500 μM) (Silbernagl and Despopoulos, 2009).

### 3.3. Selectivity of the BR ISE

The selectivity of an ISE, without a specific recognition element (an ionophore), is governed by the lipophilicity of the target ion; the sensor will respond preferentially to ions with higher lipophilic character (Buhlmann and Chen, 2012; Lindner and Pendley, 2013). The high lipophilicity of BR (Hahm et al., 1992) allows it to be sensed selectively by the ISE over other less lipophilic compounds present in blood serum. We followed a previously established method for quantifying the selectivity of the ISEs (the separate solution method) (Bakker et al., 1997; Lindner and Umezawa, 2008). The selectivity of the ISE (for BR against an interfering ion I) is commonly quantified by the logarithm of the selectivity coefficient ($logK_{BR,I}^{Pot}$, a numerical quantification of the ability of the ISE to discriminate against an interfering ion) which is given by Eq. (2) (Buhlmann and Chen, 2012). In this equation, the term $z_{BR}F/RTln10$ is the slope of the response of the sensor (*emf* vs. log concentration of BR), $E_I$ is the *emf* (mV) of the sensor in a 1-mM solution of I, and $E_{BR}$ is the *emf* of the sensor in a 1 mM solution of BR.

$$logK_{BR,\ I}^{Pot} = \frac{(E_I - E_{BR})z_{BR}F}{RTln10} \qquad (2)$$

Table 1 lists the selectivity coefficients (Eq. (2)) of the BR ISE for anions present in serum (Cl⁻, $HPO_4^{2-}$, $NO_3^-$, $HCO_3^-$, salicylate, ascorbic acid, deoxycholate, lactate, and pyruvate). Table 1 also lists the physiologically-relevant concentration range of these anions in serum. The BR ISE shows good discrimination for bilirubin over these anions (Fig. S1 shows the experimental *emf* traces), and suggests that it will be selective in the determination of free BR in human serum.

To demonstrate this selectivity, we prepared four solutions (pH 8.6, phosphate buffer) that contained all these anions (each at the maximum of their physiologically-relevant concentrations, as shown in Table 1) and different concentrations of BR and albumin. Fig. 3A shows the *emf* response of the ISE in these different solutions. Changing from the solution that contains only the interfering anions to a solution that contains 10 μM $BR^{2-}$ the *emf* immediately decreased and was stable (< 0.1 mV/min drift). When the ISE is placed into a solution of 100 μM $BR^{2-}$ the *emf* of the ISE further decreased 28 mV (as theoretically expected). The final solution contains 100 μM $BR^{2-}$ and 80 μM albumin. Albumin binds to BR (with a 1:1 stoichiometry, and a dissociation constant, $K_D = 3.7 \times 10^{-8}$ M) (Jacobsen and Brodersen, 1983; Williams et al., 2002); it is a key regulator of free BR levels in blood, and competes with cell membranes for binding to BR, and thus decreases its toxicity. Immediately after placing the ISE in this solution,

#### Table 1
The selectivity coefficient of BR ISE for BR over potentially interfering ions I ($logK_{BR,I}^{pot}$), and the physiologically-relevant concentration of anions ions in serum. The SI lists the references for each value.

| Interfering Ion | $logK_{BR,I}^{pot}$ (this work) | Physiological levels in serum |
|---|---|---|
| $BR^{2-}$ | 0 | 5–34 μM[a] |
| $HCO_3^-$ | −6.25 | 17–29 mM[a] |
| Cl⁻ | −6.11 | 98–106 mM[a] |
| $HPO_4^{2-}$ | −5.46 | 0.4–0.7 mM[a] |
| $NO_3^-$ | −4.40 | 8–68 μM[a] |
| Salicylate | −2.92 | N/A |
| Ascorbic Acid | −7.90 | 36–79 μM[b] |
| Deoxycholate | −4.33 | 5–10 μM[c] |
| Lactate | −6.47 | 0.5–1.8 mM[d] |
| Pyruvate | −6.50 | 40–120 μM[e] |

[a] (Lopez, 2013).
[b] (Levine et al., 1999).
[c] (Krishnamurthy et al., 2008).
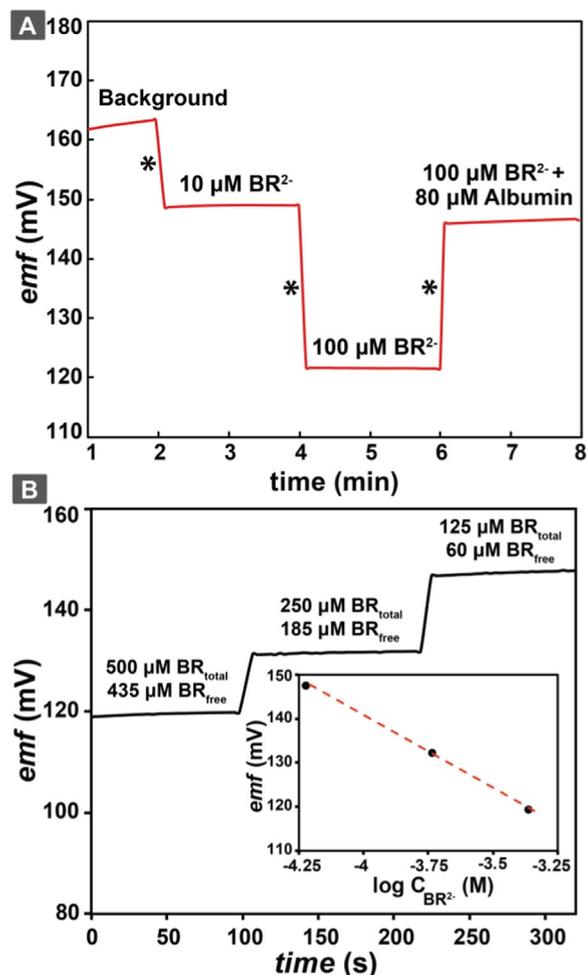[d] (Nakamura et al., 2001).
[e] (Mascini and Mazzei, 1987).

**Fig. 3.** A shows the *emf* of a BR ISE in four solutions each containing a background of 29 mM of $HCO_3^-$, 106 mM of Cl⁻, 68 μM of $NO_3^-$, 79 μM of ascorbic acid, 1.8 mM of lactate, and 120 μM of pyruvate. Asterisks show where the solutions were changed to samples containing: 10 μM BR, 100 μM BR, and 100 μM BR and 80 μM albumin. B shows the *emf* of the BR ISE in solutions (mixture of sodium phosphate buffer with pH of 8.6 and blood serum, volume ratio of 10:1) containing 500 μM, 250 μM, and 125 μM total BR. The inset shows the linear relationship of the *emf* and logarithm of concentration of free BR in this mixture (slope: − 32.8 mV/decade).

the *emf* of the BR ISE increased by 24 mV (from the measured emf of the 100 μM $BR^2$ solution), and indicates a decrease in the concentration of free BR. This experiment shows that the BR ISE is capable of selective sensing of free BR in presence of all these interfering ions, and of complexing agents such as albumin.

### 3.4. Measurements in serum

To test the effectiveness of the BR-ISE in detecting free BR in human serum, we prepared three test solutions which contained the same amount of serum (and thus the same amount of albumin), but different concentrations of BR (500 μM, 250 μM, and 125 μM). We chose these concentrations of BR because they represent the range of concentrations of BR in serum of newborns suffering from hyperbilirubinemia (Balamurugan and Berchmans, 2015). The albumin concentrations in serum range from 35 to 55 mg/mL (~500–800 μM) (Lopez, 2013); we had diluted the serum (1:10 dilution) with the phosphate buffer (pH of 8.6) to prepare the test solutions; each solution therefore contained both excess free BR, and a fixed amount of BR complexed to albumin (50–80 μM).

Fig. 3B shows the *emf* of the BR ISE in the three test solutions

containing 500 μM, 250 μM, and 125 μM total BR. Upon decreasing the initial concentration of BR from 500 μM to 250 μM (step 1), we observed a 13-mV increase in *emf* of the BR ISE. Decreasing the concentration of total BR from 250 μM to 125 μM resulted in a 15-mV increase for the second step. The calibration curve established in Fig. 2B indicates that the actual concentration of free BR in the three samples was 435 μM, 185 μM, and 60 μM and each solution contained a concentration of albumin of 65 μM (assuming a 1:1 binding of BR to albumin) (Jacobsen and Brodersen, 1983). The inset in Fig. 3B shows the *emf* had a linear relationship with the logarithm of concentration of free BR in the serum-containing solutions.

To test further the validity of using the BR-ISE in detection of free BR we prepared a solution containing 400 μM of BR and serum diluted with the phosphate pH buffer (pH of 8.6, 1:10 dilution), recorded the *emf* of the BR ISE in this solution, and converted the *emf* to the concentration of free BR using the calibration curve in Fig. 3B. The concentration of free BR in the resulting solution was 338 μM, a value that accounts for the presence of 65 μM albumin in this solution (400 μM total BR minus by the BR present in the 65 μM BR-albumin complex results in a concentration of 335 μM for free BR). This experiment demonstrates that the BR-ISE can indeed detect free BR in human serum. Moreover, the BR ISE could be used for indirect assaying of albumin (measurement of albumin through its binding to bilirubin and the change in concentration of bilirubin).

### 3.5. Translation into a paper-based device

As a demonstration of proof-of-concept of point-of-care potentiometric detection of BR, we integrated the components of the BR ISE into a paper-based potentiometric device of a design that was developed by us previously for detection of K$^+$ and Na$^+$ (Lan et al., 2014). Paper is a suitable substrate for fabrication of a point-of-care sensor because (i) it is low-cost, (ii) it can be disposed of by incineration, (iii) it can be easily patterned using wax printing technologies, and (iv) it can transport fluids through capillary wicking with no need for an external pump (Carrilho et al., 2009; Nie et al., 2010).

Fig. 4A shows a schematic of the paper-based device, which preserves all the components of the ISE shown in Fig. 1. This device consists of three layers. The first layer contains the sample and reference solutions, which are connected through the salt bridge; these zones are defined on paper using wax-printed boundaries (Carrilho et al., 2009). The second layer is the ISM which is placed over the sample zone and is sandwiched between the sample zone. The third layer (containing the inner-filling solution). The Ag/AgCl electrodes are printed on the first and third layer and enable the measurement of *emf*. Fig. 4B shows that the connection between the interfaces is similar to the conventional setup (Fig. 1A) for the potentiometric measurement.

To perform the measurement, we (i) added 15 μL of sample to the sample zone, (ii) added 15 μL of reference solution (1 M NaCl) to the reference zone, (iii) placed the ISM over the sample zone, (iv) placed the IFS layer over the ISM, (v) added 15 μL of a solution containing 0.5 mM BR and 15 mM NaCl (in a phosphate buffer with pH of 8.6) to the IFS zone, (v) placed a glass slide on top (as a weight) to hold the layers of paper in place during measurements, and connected the Ag/AgCl electrodes to the potentiometer for the measurement of *emf* (Fig. S2). Fig. 4C shows the response of this paper-based sensor to BR$^{2-}$ at the clinically-relevant concentration range of BR. The slope of *emf* vs. logarithm of concentration of BR was −22 mV/decade. This value is close to the theoretically expected Nernstian slope of −29.6 mV/decade. The limit of detection of the paper-based BR sensor was higher than that of the conventional BR ISE (100 μM vs. 0.1 μM), however, the working range of this paper-based potentiometric BR sensor is sufficient for diagnosis of hyperbilirubinemia. Worsening of the limit of detection when potentiometric sensors are integrated with paper has been reported by us and others (Hu et al., 2016a,b; Lan et al., 2014; Szűcs and Gyurcsányi, 2012). Interfacing this device with a portable and web-
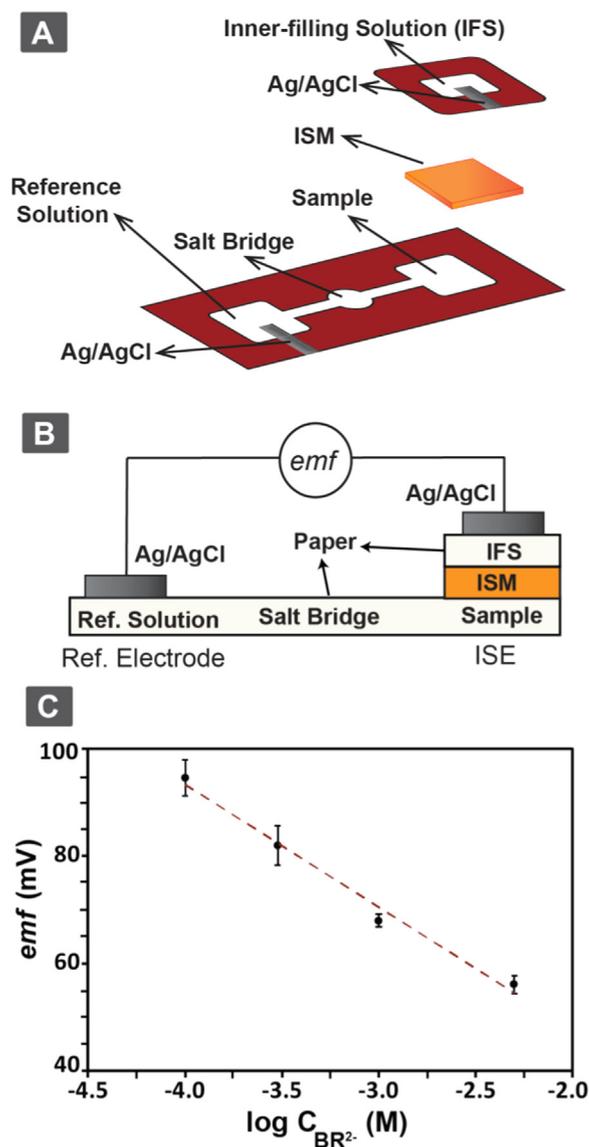


**Fig. 4.** A and B show the schematic representation of the paper-based potentiometric device. C shows the linear relationship between the *emf* and the logarithm of concentration of BR in the range of 5.0–0.10 mM (N = 7, sensor-to-sensor reproducibility was 3 mV in 1 mM BR). The dimensions of the paper-based device are 5.5 cm x 2.1 cm.

connected electrochemical detector (developed by us and others) is necessary for successful application of the sensor at the field where access to a benchtop potentiostat is not possible (Ainla et al., 2018; Dryden and Wheeler, 2015; Jeanneret et al., 2015; Lopin and Lopin, 2018; Nemiroski et al., 2014; Rowe et al., 2011).

### 4. Conclusions

To address a need for reliable diagnosis of hyperbilirubinemia in newborns in resource-limited areas, and detection of free bilirubin in the presence of complexing agents such as albumin, this work developed the first potentiometric sensor for label-free, and selective detection of free bilirubin in blood serum. Bilirubin has a doubly negative charge at physiological values of pH, and can thus be detected with a potentiometric sensor. The linear response range of the potentiometric sensor (1.0 mM–0.10 μM, at pH 8.6) is sufficiently large that it covers the normal physiological levels of bilirubin as well as levels associated with hyperbilirubinemia (up to 500 μM). We demonstrated that the

sensor selectively detects free bilirubin (and not bilirubin complexed with albumin) in the presence of common anions present in blood serum, and used this potentiometric sensor to detect free bilirubin in human blood serum directly with no need for any separation steps.

As a proof of the concept of an affordable and disposable potentiometric sensor for free bilirubin (for applications at the point-of-care or resource-limited settings), we transferred the sensing components of the bilirubin ISE to a paper-based potentiometric sensor. This paper-based sensor required only 15 μL of sample for performing the detection, and covered the clinically-relevant concentration range of bilirubin. We believe that the development of a low-cost disposable sensor can be useful in low-resource economies, where screening for jaundice in newborns currently relies on inaccurate visual methods.

The potentiometric bilirubin sensor introduces the following capabilities: (i) The sensor can be paired with a portable electrochemical detector (Ainla et al., 2018; Dryden and Wheeler, 2015; Jeanneret et al., 2015; Lopin and Lopin, 2018; Nemiroski et al., 2014; Rowe et al., 2011) for detection of bilirubin at the point-of-care and resource-limited areas, and integrated into a system of telecommunication. (ii) Because the sensor detects free bilirubin, and not bilirubin complexed to albumin, it can be incorporated into an assay for label-free detection of albumin (i.e., the amount of albumin can be detected through the decrease in the level of free bilirubin). (iii) The sensor can be integrated into a multiplexed sensor (previously developed by us) for simultaneous detection of multiple ionic components of serum (i.e., bilirubin and serum electrolytes such as $K^+$ and $Na^+$) in small volumes (Mousavi et al., 2018). The limitation of the potentiometric bilirubin sensor is that it can only detect bilirubin when it is ionic and thus it functions in the range of in pH values of 7–9 (where more than 99% of BR has a $-2$ charge). Furthermore, the somewhat complex assembly of the paper-based device will require either simplification, or users who are familiar with experimental protocols, prior to use in the field. While this work focused on demonstration of proof-of-concept and characterization of the selectivity of the potentiometric BR sensor, studying long-term stability and shelf-life of the sensor (and thus appropriate storage conditions of the sensor) are objectives of our future work.

## Acknowledgements

## Conflict of interest

The authors have no conflict of interest.

## Appendix A. Supplementary material

Supplementary data associated with this article can be found in the online version at doi:10.1016/j.bios.2018.10.055.

## References

Ahlfors, C.E., Wennberg, R.P., Ostrow, J.D., Tiribelli, C., 2009. Unbound (free) bilirubin: improving the paradigm for evaluating neonatal jaundice. Clin. Chem. 55 (7), 1288–1299.

Ainla, A., Mousavi, M.P.S., Tsaloglou, M.-N., Redston, J., Bell, J.G., Fernández-Abedul, M.T., Whitesides, G.M., 2018. Open-source potentiostat for wireless electrochemical detection with smartphones. Anal. Chem. 90 (10), 6240–6246.

Bakker, E., Bühlmann, P., Pretsch, E., 1997. Carrier-based ion-selective electrodes and bulk optodes. 1. General characteristics. Chem. Rev. 97 (8), 3083–3132.

Balamurugan, T., Berchmans, S., 2015. Non-enzymatic detection of bilirubin based on a graphene-polystyrene sulfonate composite. RSC Adv. 5 (62), 50470–50477.

Bard, A.J., Faulkner, L.R., 2009. Electrochemical Methods Fundamentals and Applications, 2nd ed. John Wiley and sons, New York.

Boiadjiev, S.E., Watters, K., Wolf, S., Lai, B.N., Welch, W.H., McDonagh, A.F., Lightner, D.A., 2004. pKa and aggregation of bilirubin: titrimetric and ultracentrifugation studies on water-soluble pegylated conjugates of bilirubin and fatty acids. Biochemistry 43 (49), 15617–15632.

Buhlmann, P., Chen, L.D., 2012. Ion-selective electrodes with ionophore-doped sensing membranes. In: Steed, J.W., Gale, P.A. (Eds.), Supramolecular Chemistry: From Molecules to Nanomaterials. John Wiley & Sons Ltd, Chichester, UK.

Carrilho, E., Martinez, A.W., Whitesides, G.M., 2009. Understanding wax printing: a simple micropatterning process for paper-based microfluidics. Anal. Chem. 81 (16), 7091–7095.

Doumas, B.T., Perry, B., Jendrzejczak, B., Davis, L., 1987. Measurement of Direct bilirubin by use of bilirubin oxidase. Clin. Chem. 33 (8), 1349–1353.

Dryden, M.D.M., Wheeler, A.R., 2015. DStat: a versatile, open-source potentiostat for electroanalysis and integration. PLOS One 10 (10), e0140349.

Erlinger, S., Arias, I.M., Dhumeaux, D., 2014. Inherited disorders of bilirubin transport and conjugation: new insights into molecular mechanisms and consequences. Gastroenterology 146 (7), 1625–1638.

Hahm, J.S., Ostrow, J.D., Mukerjee, P., Celic, L., 1992. Ionization and self-association of unconjugated bilirubin, determined by rapid solvent partition from chloroform, with further-studies of bilirubin solubility. J. Lipid Res. 33 (8), 1123–1137.

Ho, H.T., Ng, T.K., Tsui, K.C., Lo, Y.C., 2006. Evaluation of a new transcutaneous bilirubinometer in Chinese newborns. Archives of disease in childhood. Fetal Neonatal Ed. 91 (6), F434–F438.

Hu, J., Stein, A., Bühlmann, P., 2016a. A disposable planar paper-based potentiometric ion-sensing platform. Angew. Chem. Int. Ed. 55 (26), 7544–7547.

Hu, J., Stein, A., Bühlmann, P., 2016b. Rational design of all-solid-state ion-selective electrodes and reference electrodes. TrAC, Trends Anal. Chem. 76, 102–114.

Jacobsen, J., Brodersen, R., 1983. albumin-bilirubin binding mechanism - Kinetic and spectroscopic studies of binding of bilirubin and Xanthobilirubic acid to human-serum albumin. J. Biol. Chem. 258 (10), 6319–6326.

Jeanneret, S., Crespo, G.A., Ghahraman Afshar, M., Bakker, E., 2015. GalvaPot, a custom-made combination galvanostat/potentiostat and high impedance potentiometer for decentralized measurements of ionophore-based electrodes. Sens. Actuators B: Chem. 207, 631–639.

Joseph, W., Mebmet, O., 1990. A polishable amperometric biosensor for bilirubin. Electroanalysis 2 (8), 647–650.

Kapitulnik, J., 2004. Bilirubin: an endogenous product of heme degradation with both cytotoxic and cytoprotective properties. Mol. Pharmacol. 66 (4), 773–779.

Keahey, P.A., Simeral, M.L., Schroder, K.J., Bond, M.M., Mtenthaonnga, P.J., Miros, R.H., Dube, Q., Richards-Kortum, R.R., 2017. Point-of-care device to diagnose and monitor neonatal jaundice in low-resource settings. Proc. Natl. Acad. Sci. USA 114 (51), E10965–E10971.

Krishnamurthy, K., Wang, G.H., Rokhfeld, D., Bieberich, E., 2008. Deoxycholate promotes survival of breast cancer cells by reducing the level of pro-apoptotic ceramide. Breast Cancer Res. 10 (6).

Lan, W.-J., Zou, X.U., Hamedi, M.M., Hu, J., Parolo, C., Maxwell, E.J., Bühlmann, P., Whitesides, G.M., 2014. Paper-based potentiometric ion sensing. Anal. Chem. 86 (19), 9548–9553.

Levine, M., Rumsey, S.C., Daruwala, R., Park, J.B., Wang, Y.H., 1999. Criteria and recommendations for vitamin C intake. JAMA-J. Am. Med. Assoc. 281 (15), 1415–1423.

Li, X., Rosenzweig, Z., 1997. A fiber optic sensor for rapid analysis of bilirubin in serum. Anal. Chim. Acta 353 (2), 263–273.

Lindner, E., Gyurcsányi, R.E., 2009. Quality control criteria for solid-contact, solvent polymeric membrane ion-selective electrodes. J. Solid State Electrochem. 13, 51.

Lindner, E., Pendley, B.D., 2013. A tutorial on the application of ion-selective electrode potentiometry: an analytical method with unique qualities, unexplored opportunities and potential pitfalls; Tutorial. Anal. Chim. Acta 762, 1–13.

Lindner, E., Umezawa, Y., 2008. Performance evaluation criteria for preparation and measurement of macro- and microfabricated ion-selective electrodes (IUPAC technical report). Pure Appl. Chem. 80 (1), 85.

Lopez-Velazquez, J.A., Chavez-Tapia, N.C., Ponciano-Rodriguez, G., Sanchez-Valle, V., Caldwell, S.H., Uribe, M., Mendez-Sanchez, N., 2014. Bilirubin alone as a biomarker for short-term mortality in acute-on-chronic liver failure: an important prognostic indicator. Ann. Hepatol. 13 (1), 98–104.

Lopez, J., Burtis, Carl A., Ashwood, Edward R., Bruns, David E., 2013. Tietz textbook of clinical chemistry and molecular diagnosis (5th edition). Indian J. Clin. Biochem. 28 (1), 104–105.

Lopin, P., Lopin, K.V., 2018. PSoC-stat: a single chip open source potentiostat based on a programmable system on a chip. PLOS One 13 (7), e0201353.

Lu, C., Lin, J.-M., Huie, C.W., 2004. Determination of total bilirubin in human serum by chemiluminescence from the reaction of bilirubin and peroxynitrite. Talanta 63 (2), 333–337.

Ma, G., Lin, J., Cai, W., Tan, B., Xiang, X., Zhang, Y., Zhang, P., 2014. Simultaneous determination of bilirubin and its glucuronides in liver microsomes and recombinant UGT1A1 enzyme incubation systems by HPLC method and its application to bilirubin glucuronidation studies. J. Pharm. Biomed. Anal. 92, 149–159.

Mascini, M., Mazzei, F., 1987. Amperometric sensor for pyruvate with immobilized pyruvate oxidase. Anal. Chim. Acta 192 (1), 9–16.

Maurer-Jones, M.A., Mousavi, M.P.S., Chen, L.D., Buhlmann, P., Haynes, C.L., 2013. Characterization of silver ion dissolution from silver nanoparticles using fluorous-phase ion-selective electrodes and assessment of resultant toxicity to shewanella

oneidensis. Chem. Sci. 4 (6), 2564–2572.

Mousavi, M.P.S., Ainla, A., Tan, E.K.W., K. Abd El-Rahman, M., Yoshida, Y., Yuan, L., Sigurslid, H.H., Arkan, N., Yip, M.C., Abrahamsson, C.K., Homer-Vanniasinkam, S., Whitesides, G.M., 2018. Ion sensing with thread-based potentiometric electrodes. Lab Chip. 18 (15), 2279–2290.

Mousavi, M.P.S., Gunsolus, I.L., Pérez De Jesús, C.E., Lancaster, M., Hussein, K., Haynes, C.L., Bühlmann, P., 2015. Dynamic silver speciation as studied with fluorous-phase ion-selective electrodes: effect of natural organic matter on the toxicity and speciation of silver. Sci. Total Environ. 537, 453–461.

Moyer, V.A., Ahn, C., Sneed, S., 2000. Accuracy of clinical judgment in neonatal jaundice. Arch. Pediatr. Adolesc. Med. 154 (4), 391–394.

Nakamura, H., Murakami, Y., Yokoyama, K., Tamiya, E., Karube, I., 2001. A compactly integrated flow cell with a chemiluminescent FIA system for determining lactate concentration in serum. Anal. Chem. 73 (2), 373–378.

Nemiroski, A., Christodouleas, D.C., Hennek, J.W., Kumar, A.A., Maxwell, E.J., Fernández-Abedul, M.T., Whitesides, G.M., 2014. Universal mobile electrochemical detector designed for use in resource-limited applications. Proc. Natl. Acad. Sci. USA 111 (33), 11984–11989.

Nie, Z., Fung, Y.S., 2008. Microchip capillary electrophoresis for frontal analysis of free bilirubin and study of its interaction with human serum albumin. Electrophoresis 29 (9), 1924–1931.

Nie, Z., Nijhuis, C.A., Gong, J., Chen, X., Kumachev, A., Martinez, A.W., Narovlyansky, M., Whitesides, G.M., 2010. Electrochemical sensing in paper-based microfluidic devices. Lab Chip. 10 (4), 477–483.

Novell, M., Parrilla, M., Crespo, G.A., Rius, F.X., Andrade, F.J., 2012. Paper-based ion-selective potentiometric sensors. Anal. Chem. 84 (11), 4695–4702.

Rand, R.N., Pasqua, Ad, 1962. A new diazo method for the determination of bilirubin.

Clin. Chem. 8 (6), 570–578.

Rowe, A.A., Bonham, A.J., White, R.J., Zimmer, M.P., Yadgar, R.J., Hobza, T.M., Honea, J.W., Ben-Yaacov, I., Plaxco, K.W., 2011. CheapStat: an open-source, "do-it-yourself" potentiostat for analytical and educational applications. PLOS One 6 (9), e23783.

Ruecha, N., Chailapakul, O., Suzuki, K., Citterio, D., 2017. Fully inkjet-printed paper-based potentiometric ion-sensing devices. Anal. Chem. 89 (19), 10608–10616.

Ryoichi, F., Mathias, H., Elke, S., T, N.A., M, Z.U., Matthias, S., 2018. Systemic regulation of bilirubin homeostasis: potential benefits of hyperbilirubinemia. Hepatology 67 (4), 1609–1619.

Santhosh, M., Chinnadayyala, S.R., Kakoti, A., Goswami, P., 2014. Selective and sensitive detection of free bilirubin in blood serum using human serum albumin stabilized gold nanoclusters as fluorometric and colorimetric probe. Biosens. Bioelectron. 59, 370–376.

Shoham, B., Migron, Y., Riklin, A., Willner, I., Tartakovsky, B., 1995. A bilirubin biosensor based on a multilayer network enzyme electrode. Biosens. Bioelectron. 10 (3), 341–352.

Silbernagl, S., Despopoulos, A., 2009. Color Atlas of Physiology. Thieme, Stuttgart.

Szűcs, J., Gyurcsányi, R.E., 2012. Towards protein assays on paper platforms with potentiometric detection. Electroanalysis 24 (1), 146–152.

Williams, K.R., Adhyaru, B., Pierce, R., Schulman, S.G., 2002. The binding constant for complexation of bilirubin to bovine serum albumin – an experiment for the biophysical chemistry laboratory. J. Chem. Edu. 79 (1), 115–116.

Yamanouchi, I., Yamauchi, Y., Igarashi, I., 1980. Trancutaneous Bilirubinometry. Preliminary Studies of Non-Invasive Transcutaneous Bilirubin Meter in the Okayama National Hospital.

Yang, Z., Yan, J., Zhang, C., 2012. Piezoelectric detection of bilirubin based on bilirubin-imprinted titania film electrode. Anal. Biochem. 421 (1), 37–42.